Acta Cryst. (1998). B**54**, 494–502

Structural Investigations of the Phase Transitions of Tetramethylammonium Sulfate

Michael Malchus and Martin Jansen*

Institut für Anorganische Chemie der Universität Bonn, Gerhard-Domagk-Strasse 1, 53121 Bonn, Germany. E-mail: mjansen@snchemie2.chemie.uni-bonn.de

(*Received 15 July 1997; accepted 28 November 1997*)

Abstract

Tetramethylammonium sulfate, $[N(CH_3)_4]_2SO_4$, was prepared in high purity *via* ion exchange. Two reversible first-order phase transitions at 263 ± 3 and 462 ± 3 K have been established by differential thermal analysis and temperature-dependent X-ray powder diffraction. Crystal structure determinations at 223 and 293 K reveal completely ordered sulfate and tetramethylammonium tetrahedra for the low-temperature modification, while at room temperature half of the sulfate groups are orientationally disordered. The space groups are $P4_2/nmc$ with a = 7.5355 (9), c = 10.9910 (14) Å and Z = 2 [$wR(F^2)$ = 0.089 for 239 independent reflections] and $P4/nbm$ with a = 10.8948 (9), c = 10.789 (2) Å and Z = 4 [$wR(F^2)$ = 0.118 for 792 independent reflections], respectively. Powder patterns, as recorded at 473 K by the Guinier–Simon X-ray technique, show that the high-temperature modification is cubic face-centered with a = 11.026 (2) Å and is likely to contain only free-rotating tetrahedra. The common aristotype of all three modifications is the fluorite-type structure. An examination of group–subgroup relations is made.

1. Introduction

Tetramethylammonium salts are of general interest in preparative chemistry. Their enhanced solubility in aprotic solvents in comparison to their corresponding alkali metal salts, as well as the higher reactivity due to a lower degree of solvatization of their anions in solutions of unpolar solvents, make them a powerful and versatile tool. For example, the availability of anhydrous $[N(CH_3)_4]F$ (Christe *et al.*, 1990) allowed the first access to a PF_4^- salt (Christe *et al.*, 1994) or to highly coordinated anions such as XeF_5^- (Christe *et al.*, 1991). Nevertheless, knowledge about the crystal chemistry of tetraalkylammonium salts is still limited. This is true particularly for tetraoxo complex salts of the A_2B type, such as $[N(CH_3)_4]_2SO_4$.

The syntheses of tetramethylammonium salts can be achieved by several well established methods such as: (i) neutralizing a suitable acid with $[N(CH_3)_4]OH$, (ii) precipitation by mixing soluble $[N(CH_3)_4]X$ and Na_2MX_4 or MX_2 salts in suitable solvents, (iii) alkylation of amines *via* the Hoffmann reaction {$N(CH_3)_3 + (CH_3)X \rightarrow [N(CH_3)_4]X$} or (iv) displacement of the more weakly basic ammonia from aqueous solutions of ammonium salts as per the equation: $[N(CH_3)_4]OH + NH_4X \rightarrow [N(CH_3)_4]X + H_2O + NH_3$ (Markowitz, 1957). Synthesis *via* the equation in (iii) is of interest as a solvent-free synthesis of tetramethylammonium salts (Albert & Jansen, 1995). In certain cases special synthetic routes have been applied. The sulfate, for instance, may be synthesized by oxidation of $[N(CH_3)_4]I$ with aqueous $K_2S_2O_8$ solutions (Husain & Singh, 1984).

$[N(CH_3)_4]_2SO_4$ has been characterized recently by ^1H NMR, differential thermal analysis and X-ray powder diffraction techniques (Sato *et al.*, 1995). However, no single crystal data were given and the temperature range applied for thermal analysis was rather limited (105–400 K).

In this paper we report on a detailed thermal analysis, IR and Raman spectroscopy, and crystal structure determinations of two of the polymorphic modifications of $[N(CH_3)_4]_2SO_4$.

2. Experimental

Tetramethylammonium sulfate as purchased, as well as prepared by neutralizing $[N(CH_3)_4]HSO_4$ or H_2SO_4 with $[N(CH_3)_4]OH$, was found to be impure. Samples of improved purity were obtained *via* ion exchange, which has the advantage of avoiding carbonate impurities from the CO_2 absorbing $[N(CH_3)_4]OH$.

A solution of Na_2SO_4 (Riedel de Häen, 13464) in bidistilled water is exchanged with $[N(CH_3)_4]^+$-loaded cation exchange resin Amberlyst 15 (Merck, 15635) {acidic form loaded with $[N(CH_3)_4]OH.5H_2O$ (Fluka, 87741) in bidistilled water and washed}. After filtration the product is isolated by freeze-drying and then handled strictly under dry argon. Powder samples were sealed in argon-filled capillaries. Single crystals have been grown by slow diffusion of acetylacetate into a methanolic solution of $[N(CH_3)_4]_2SO_4$. After removing the solvent, suitable crystals were checked optically with a polarizing light microscope, sealed in argon-filled capillaries and tested by X-ray oscillation photographs at room temperature.

Crystal data collection was performed on an Enraf–Nonius CAD-4 automatic four-circle diffractometer

ISSN 0108-7681

Table 1. *Experimental details*

	Low temperature	Room temperature
Crystal data		
Chemical formula	$2(C_4H_{12}N^+)(SO_4^{2-})$	$2(C_4H_{12}N^+)(SO_4^{2-})$
Chemical formula weight	244.35	244.35
Cell setting	Tetragonal	Tetragonal
Space group	$P4_2/nmc$	$P4/nbm$
a (Å)	7.5355 (9)	10.8948 (9)
b (Å)	7.5355 (9)	10.8948 (9)
c (Å)	10.9910 (14)	10.789 (2)
V (Å^3)	624.11 (14)	1280.6 (3)
Z	2	4
D_x (Mg m^{-3})	1.300	1.267
Radiation type	Mo $K\alpha$	Mo $K\alpha$
Wavelength (Å)	0.7107	0.7107
No. of reflections for cell parameters	25	25
θ range (°)	4.6–14.4	3.2–23.3
μ (mm^{-1})	0.259	0.252
Temperature (K)	223 (2)	293 (2)
Crystal form	Tetragonal bipyramid	See Fig. 4
Crystal size (mm)	0.19 × 0.15 × 0.15	0.38 × 0.3 × 0.24
Crystal color	Colorless	Colorless
Data collection		
Diffractometer	Enraf–Nonius CAD-4	Enraf–Nonius CAD-4
Data collection method	ω scans	ω–θ scans
Absorption correction	None	Numerical with FACE cards
T_{min}	–	0.932
T_{max}	–	0.962
No. of measured reflections	1532	3770
No. of independent reflections	239	792
No. of observed reflections	219	701
Criterion for observed reflections	$I > 2\sigma(I)$	$I > 2\sigma(I)$
R_{int}	0.0541	0.0151
θ_{max} (°)	22.92	27.47
Range of h, k, l	$-8 \rightarrow h \rightarrow 7$ $-1 \rightarrow k \rightarrow 7$ $-10 \rightarrow l \rightarrow 10$	$0 \rightarrow h \rightarrow 12$ $0 \rightarrow k \rightarrow 15$ $0 \rightarrow l \rightarrow 15$
No. of standard reflections	2	3
Frequency of standard reflections (min)	60	60
Refinement		
Refinement on	F^2	F^2
$R[F^2 > 2\sigma(F^2)]$	0.0364	0.0667
$wR(F^2)$	0.0888	0.1181
S	1.194	1.344
No. of reflections used in refinement	239	792
No. of parameters used	39	81
H-atom treatment	Only coordinates of H atoms refined	Only coordinates of H atoms refined
Weighting scheme	$w = 1/[\sigma^2(F_o^2) + (0.0454P)^2 + 0.3184P]$, where $P = (F_o^2 + 2F_c^2)/3$	$w = 1/[\sigma^2(F_o^2) + (0.0087P)^2 + 0.9623P]$, where $P = (F_o^2 + 2F_c^2)/3$
$(\Delta/\sigma)_{max}$	<0.001	<0.001
$\Delta\rho_{max}$ (e Å^{-3})	0.219	0.364
$\Delta\rho_{min}$ (e Å^{-3})	−0.209	−0.283
Extinction method	None	None
Source of atomic scattering factors	*International Tables for X-ray Crystallography* (1974, Vol. C, Tables 4.2.6.8 and 6.1.1.4)	*International Tables for X-ray Crystallography* (1974, Vol. C, Tables 4.2.6.8 and 6.1.1.4)
Computer programs		
Data collection	*CAD*-4 software (Enraf–Nonius, 1989)	*CAD*-4 software (Enraf–Nonius, 1989)
Cell refinement	*CELDIM* (Enraf–Nonius, 1989)	*CELDIM* (Enraf–Nonius, 1989)
Data reduction	*CADSHEL* (Kopf & Ruebcke, 1993)	*CADSHEL* (Kopf & Ruebcke, 1993)
Structure solution	*SHELXS*86 (Sheldrick, 1985)	*SHELXS*86 (Sheldrick, 1985)
Structure refinement	*SHELXL*93 (Sheldrick, 1993)	*SHELXL*93 (Sheldrick, 1993)

Table 2. *Vibrational spectra of solid* $[N(CH_3)_4]_2SO_4$

Observed frequencies (cm^{-1})		Assignments (point group)	
IR	Raman	$N(CH_3)_4$ (T_d)	SO_4 (T_d)
3479 w		$\nu CH_3 + \nu_{19}$	
3387 w		$\nu CH_3 + \nu_8$	
3019 s	3015	$\nu_{13}(F_2)\nu_{as}CH_3$	
	2980	$\nu_5(E)\nu_{as}CH_3$	
2939 w	2927	$\nu_{14}(F_2)\nu_{sym}CH_3$	
2828 w	2836	$\nu_1(A_1)\nu_{sym}CH_3$	
2625 w		+ combination bands	
2531 w			
2389 w			
2041 w			
1507 s		$\nu_{15}(F_2)\delta_{as}CH_3$	
1488 m	1482	$\nu_6(E)\delta_{as}CH_3$	
1432 w	1427	$\nu_{16}(F_2)\delta_{sym}CH_3$	
1313 w	1302	$\nu_{17}(F_2)CH_3$ rock	
	1208		$2\nu_4(F_2)$
	1099		
1081 vs	1082		$\nu_3(F_2)\nu_dSO_4$
967 s	963	$\nu_{18}(F_2)\nu_{as}C_4N$	$\nu_1(A_1)\nu_sSO_4$
949 s		$2\nu_{19}$	
	760	$\nu_3(A_1)\nu_{sym}C_4N$	
609 s	609		$\nu_4(F_2)\delta_dSO_4$
468 s	460	$\nu_{19}(F_2)\delta C_4N$	$\nu_2(E)\delta_dSO_4$
	438		
	383	$\nu_8(E)\delta C_4N$	

(graphite-monochromated Mo $K\alpha$ radiation, λ = 0.71069 Å) with cooling equipment (Enraf–Nonius FR558-S). Lattice parameters were determined by least-squares refinement of 25 accurately centered reflections. For data reduction, structure solution by direct methods and final refinement by full-matrix least-squares methods the programs *CADSHEL* (Kopf & Ruebcke, 1993), *SHELXS*86 (Sheldrick, 1985) and *SHELXL*93 (Sheldrick, 1993) were used. Raw data intensities of the room-temperature phase were corrected for absorption by numerical methods using *SHELX*76 (Sheldrick, 1976). For the low-temperature raw data no absorption correction was applied [μ(Mo $K\alpha$) = 0.26 mm^{-1}]. Structure plots were generated using the programs *KPLOT* (Hundt, 1979) and *ORTEP* (Johnson, 1971). For data collection of the low-temperature modification a single crystal of $[N(CH_3)_4]_2SO_4$ was cooled from 293 to 223 K with a rate of 10 K h^{-1}. Crystal data for $[N(CH_3)_4]_2SO_4$ at 223 and 293 K, together with the experimental parameters, are given in Table 1.

Powder diffraction patterns at constant temperatures were recorded using a Stoe Stadi-P powder diffractometer (Cu $K\alpha_1$, germanium monochromated, PSD, position-sensitive detector) with cooling equipment. A Guinier–Simon camera (Enraf–Nonius FR533, Cu $K\alpha_1$, Johansson monochromator) was used to obtain temperature-dependent powder patterns. All powder data were corrected using low quartz as an external standard.

For solid-state IR spectra (Bruker, Fourier-transform IR IFS 113v), $[N(CH_3)_4]_2SO_4$ was dispersed and pressed into KBr pellets in an argon-filled glove-box; for solid-state Raman spectra (Bruker, Fourier-transform Raman RFS 100 with Nd-YAG laser, λ = 1064 nm), capillaries were filled and sealed.

Differential thermal analysis (DTA), thermogravimetric measurements (TG) and mass spectroscopy of the evolved gases (MS) were carried out simultaneously in a thermal analyzer (Netzsch STA system 409/429–403) with a heating rate of 5 K min^{-1}. The glass crucibles were filled under dry argon, sealed and opened just before measurement in dry argon as a carrier gas.

3. IR and Raman spectroscopy

In order to reveal information about the purity of the samples and the distortion of the $[N(CH_3)_4]^+$ cation, vibrational spectra were collected. Fig. 1 shows the IR and Raman spectra of solid $[N(CH_3)_4]_2SO_4$. Observed frequencies and their assignments are summarized in Table 2. The assignments and mode descriptions follow those published by Berg (1978) and Christe *et al.* (1990) for $[N(CH_3)_4]^+$ and Nakamoto (1986) for SO_4^{2-}. For a free $[N(CH_3)_4]^+$ cation with T_d symmetry, 19 fundamental vibrations classified as $3A_1 + A_2 + 4E + 4F_1 + 7F_2$ are allowed. Only vibrations with F_2 symmetry are IR-

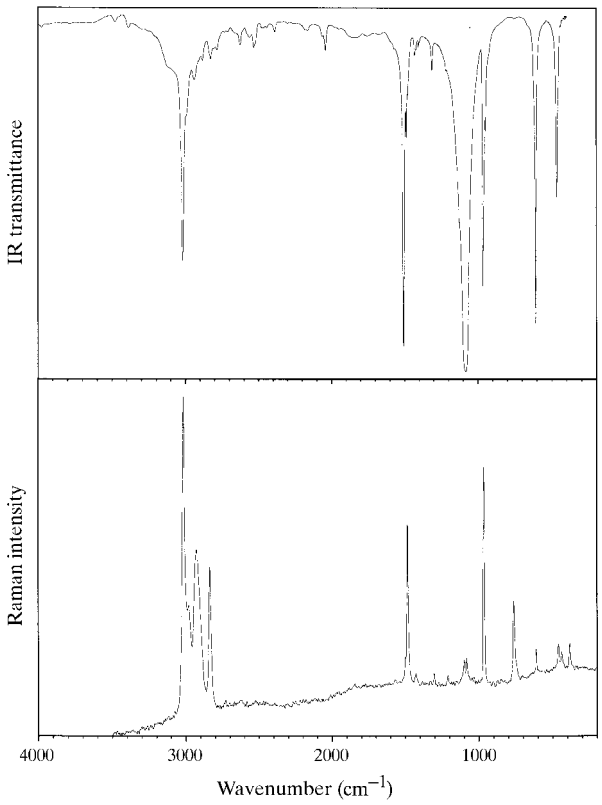

Fig. 1. IR and Raman spectra of solid $[N(CH_3)_4]_2SO_4$.

active; the A_2 and F_1 vibrations of the unperturbed ion cannot be observed either in the Raman or the IR spectra. In the solid state the number of fundamentals can increase and the selection rules be violated due to effects such as distortion of the $[N(CH_3)_4]^+$ tetrahedron, site symmetries lower than T_d and factor group splittings. For a free SO_4^{2-} anion, four fundamental vibrations classified as $A_1 + E + 2F_2$ are allowed. Again, only vibrations with F_2 symmetry are IR-active, but here all vibrations are Raman-active. Kabisch (1980) demonstrated that a decreasing ν_8/ν_{19} Raman intensity ratio is a measure for the degree of distortion of a $[N(CH_3)_4]^+$ cation. For $[N(CH_3)_4]_2SO_4$, this ratio indicates a negligible distortion of the cation. Furthermore, no forbidden A_2 and F_1 vibrations are visible. Therefore, no major deviation from the ideal T_d symmetry of the $[N(CH_3)_4]^+$ cation is detectable by vibrational spectroscopy.

4. Thermal analysis

The thermal behavior of $[N(CH_3)_4]_2SO_4$ was investigated between 103 and 773 K. Temperature-dependent Guinier–Simon X-ray measurements in the temperature range from 103 K to decomposition of the sulfate show two reversible phase transitions at 263 ± 3 and 458 ± 3 K. Coupled thermogravimetric and differential thermal analysis measurements, combined with mass spectroscopy of the evolved gases, show an endothermic effect at 462 ± 3 K without loss of mass relating to the first-order structural phase transition (see Fig. 2). The

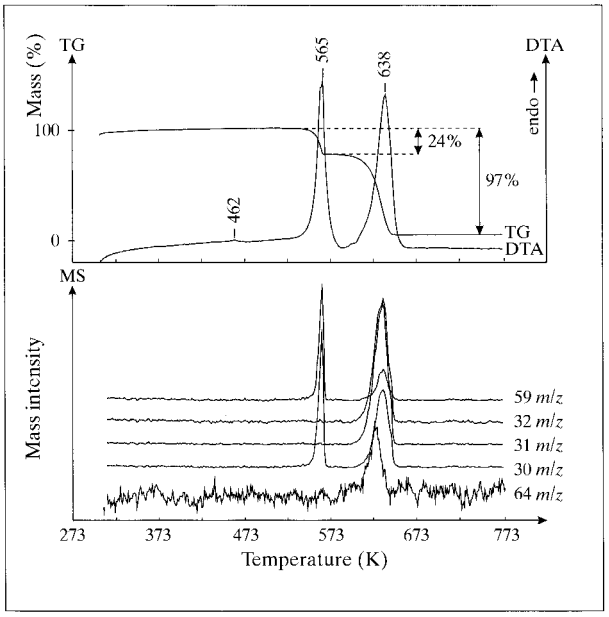

Fig. 2. Coupled TG/DTA curves combined with temperature-dependent mass intensities. Scan rate: 5 K min^{-1}; carrier gas: argon.

Table 3. *Fractional atomic coordinates and equivalent isotropic displacement parameters (Å²) for $[N(CH_3)_4]_2SO_4$ at 223 K*

$U_{eq} = (1/3)\Sigma_i\Sigma_j U^{ij} a^i a^j \mathbf{a}_i.\mathbf{a}_j.$

	x	*y*	*z*	U_{eq}
S1	0.0	0.0	0.0	0.0152 (6)
O1	0.0	0.1582 (3)	0.0768 (2)	0.0398 (8)
N1	1/2	0.0	0.1938 (3)	0.0186 (9)
C1	0.6621 (4)	0.0	0.2722 (3)	0.0226 (8)
C2	1/2	0.1626 (4)	0.1155 (3)	0.0290 (9)
H1	0.653 (2)	−0.103 (3)	0.3239 (15)	0.024 (6)
H2	0.763 (5)	0.0	0.219 (3)	0.033 (9)}
H3	0.400 (3)	0.162 (3)	0.0667 (15)	0.033 (6)
H4	1/2	0.258 (4)	0.169 (2)	0.017 (8)

sulfate decomposes passing two endothermic steps at 565 ± 3 and 638 ± 3 K. First 1 mol of $N(CH_3)_3$ [59 *m/z*] evolves (loss of mass: 24%, calc. 24.2%). The decomposition of the intermediate $[N(CH_3)_4]SO_3(OCH_3)$ is more complicated and masses of SO_2 [64 *m/z*], $N(CH_3)_3$ [59 *m/z*], CO_2 [44 *m/z*], CH_3OH [32 *m/z*] and its fragment $CH_3]^+$ [31 *m/z*] were detected. Additionally, fragments of $N(CH_3)_3$ [58 *m/z*, 42 *m/z*, 30 *m/z*, 15 *m/z*] show increasing intensity at both decomposition steps. In the crucible remains a small amount of a black residue. Selected masses are shown in Fig. 2. A simple decomposition of $[N(CH_3)_4]_2SO_4$ to $N(CH_3)_3$ and dimethylsulfate is unlikely to occur because dimethylsulfate decomposes at its boiling point, 461 K (Gerhartz, 1987).

$$[N(CH_3)_4]_2SO_4 \rightarrow [N(CH_3)_4]SO_3(OCH_3) + N(CH_3)_3 \quad (1a)$$

$$[N(CH_3)_4]SO_3(OCH_3) \rightarrow N(CH_3)_3 + SO_2 + CH_3OH + CH_2O \quad (1b)$$

The phase transition temperatures found in this work do not agree with those reported by Sato *et al.* (1995), who detected one reversible thermal effect at 279 K. A further heat anomaly at 273 K on heating is attributed to some moisture left in the sample.

5. Crystal structure of the tetragonal low-temperature phase

Powder diffraction data of the low-temperature form (LT), measured on a diffractometer at 243 K and a cooling Guinier–Simon camera, can be indexed tetragonally with $a = 7.5461$ (8) and $c = 10.997$ (2) Å.

The crystal structure was solved by applying single crystal data and using direct methods; all atoms, including H atoms, were localized by Fourier methods. The refinement of the atomic parameters was based on F^2, first using isotropic for all atoms and finally anisotropic atomic displacement parameters for all non-H

Table 4. *Selected geometric parameters (Å, °) for $[N(CH_3)_4]_2SO_4$ at 223 K*

S1—O1	1.461 (2)	C1—H2	0.96 (4)
N1—C1	1.495 (3)	C2—H3	0.92 (2)
N1—C2	1.497 (3)	C2—H4	0.93 (3)
C1—H1	0.96 (2)		
$O1^{i}$—S1—O1	109.51 (9)	N1—C1—H2	107.4 (17)
$O1^{i}$—S1—$O1^{ii}$	109.4 (2)	H1—C1—H2	114.4 (14)
C1—N1—$C1^{iii}$	109.6 (3)	N1—C2—H3	109.2 (14)
C1—N1—$C2^{iii}$	109.36 (9)	N1—C2—H4	105.4 (18)
$C2^{iii}$—N1—C2	109.8 (3)	H3—C2—H4	112.1 (16)
N1—C1—H1	106.5 (12)		

Symmetry codes: (i) $-y, x, -z$; (ii) $y, -x, -z$; (iii) $1-x, -y, z$.

atoms. Atomic coordinates and equivalent isotropic displacement parameters for LT-$[N(CH_3)_4]_2SO_4$ are given in Table 3, and selected bonds lengths and angles in Table 4. Fig. 3 shows the unit cell of LT-$[N(CH_3)_4]_2SO_4$.†

The structure consists of regular and isolated SO_4^{2-} and $[N(CH_3)_4]^+$ tetrahedra. Bond lengths and angles show no significant deviations from values expected for the SO_4^{2-} and $[N(CH_3)_4]^+$ tetrahedra. The cation/anion packing is related to a tetragonally distorted Li_2O-type structure.

6. Crystal structure of the tetragonal room-temperature phase

Powder diffraction data for the room-temperature phase (RT) of $[N(CH_3)_4]_2SO_4$ can be indexed tetragonally with $a = 10.890$ (2) and $c = 10.791$ (3) Å. This is in agreement with the indexing proposed by Sato *et al.* (1995).

The crystal structure was solved by applying single-crystal data and using direct methods; all atoms including H atoms were localized by Fourier methods. Owing to the size and the rather anisotropic form of the crystal selected, a numerical absorption was applied (see Fig. 4). The refinement of atomic parameters was based on F^2, first using isotropic for all atoms and finally anisotropic atomic displacement parameters for all non-H atoms. Atomic coordinates and equivalent isotropic displacement parameters for RT-$[N(CH_3)_4]_2SO_4$ are given in Table 5, selected bond lengths and angles in Table 6.

The $[N(CH_3)_4]^+$ cation again is well defined and regular, which is in agreement with the data from the vibrational spectra. There are two different sulfate positions. The sulfate ion at $0,\frac{1}{2},0$ is well fixed and regular; the second SO_4^{2-} anion at $0,0,\frac{1}{2}$, however, is orientationally disordered. A reasonable fit of calculated and observed F^2 was achieved by refining a split atom model (*cf.* Table 5). In this latter case the S—O bond length was restrained to 1.45 Å. Fig. 5 shows the

† Lists of atomic coordinates, anisotropic displacement parameters and structure factors, and the numbered intensity of each measured point on the profile have been deposited with the IUCr (Reference: JZ0003). Copies may be obtained through The Managing Editor, International Union of Crystallography, 5 Abbey Square, Chester CH1 2HU, England.

Table 5. *Fractional atomic coordinates and equivalent isotropic displacement parameters (Å²) for $[N(CH_3)_4]_2SO_4$ at 293 K*

$U_{eq} = (1/3)\Sigma_i\Sigma_j U^{ij} a^i a^j \mathbf{a}_i.\mathbf{a}_j$.

	x	y	z	U_{eq}
S1	0.0	1/2	0.0	0.0246 (3)
O1	0.0775 (2)	0.4225 (2)	−0.0772 (3)	0.0591 (9)
N1	0.2193 (2)	0.2807 (2)	0.2515 (2)	0.0308 (6)
C1	0.1412 (3)	0.2007 (3)	0.1717 (3)	0.0479 (7)
C2	0.2980 (2)	0.2020 (2)	0.3320 (4)	0.0427 (9)
C3	0.1399 (3)	0.3601 (3)	0.3300 (4)	0.0489 (10)
S2	0.0	0.0	1/2	0.0371 (4)
O3	0.025 (4)	0.1009 (19)	0.5604 (17)	0.210 (16)
O4	0.0	0.0	0.6382 (11)	0.105 (7)
O5	0.0	0.1370 (12)	1/2	0.073 (5)
H1	0.195 (3)	0.149 (4)	0.118 (3)	0.071 (11)
H2	0.094 (3)	0.146 (3)	0.223 (2)	0.070 (11)
H3	0.090 (3)	0.249 (3)	0.119 (3)	0.066 (10)
H4	0.344 (3)	0.255 (3)	0.386 (2)	0.045 (8)
H5	0.349 (3)	0.151 (3)	0.281 (4)	0.046 (12)
H6	0.090 (3)	0.410 (3)	0.281 (4)	0.052 (12)
H7	0.190 (3)	0.408 (3)	0.387 (2)	0.061 (10)

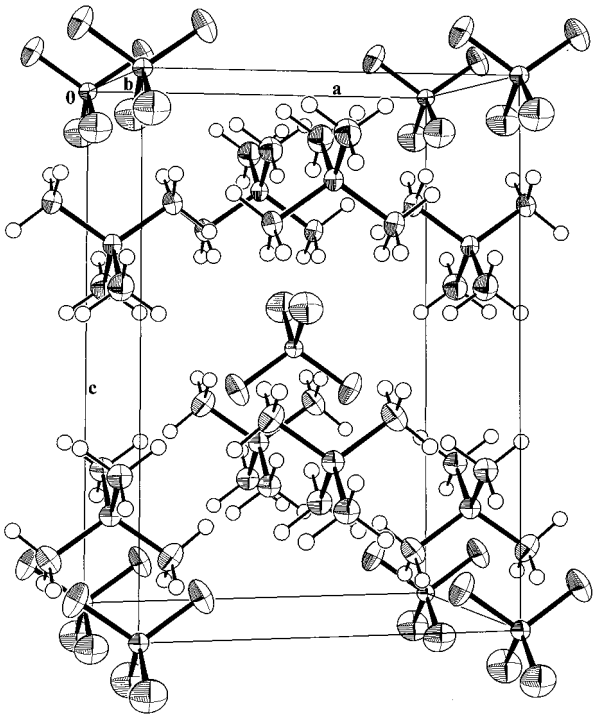

Fig. 3. *ORTEP*II (Johnson, 1971) plot (50% probability level) of the tetragonal LT-$[N(CH_3)_4]_2SO_4$ unit cell.

Table 6. *Selected geometric parameters (Å, °) for $[N(CH_3)_4]_2SO_4$ at 293 K*

S1—O1^{i}	1.456 (3)	C2—H4	0.96 (3)
S1—O1^{ii}	1.456 (3)	C2—H5	0.96 (4)
S1—O1^{iii}	1.456 (3)	C3—H6	0.93 (4)
N1—C1^{iv}	1.492 (3)	C3—H7	0.98 (3)
N1—C1	1.492 (3)	S2—O3	1.307 (14)
C1—H1	1.00 (4)	S2—O4	1.491 (12)
C1—H2	0.96 (3)	S2—O5	1.492 (13)
C1—H3	0.95 (4)		
O1^{i}—S1—O1^{iii}	109.08 (13)	N1—C1—H3	111 (2)
O1^{ii}—S1—O1^{iii}	110.2 (3)	H1—C1—H3	108 (2)
C3—N1—C2	109.7 (3)	H2—C1—H3	112 (3)
C3—N1—C1	109.6 (2)	N1—C2—H4	108.0 (18)
C2—N1—C1	109.2 (2)	N1—C2—H5	109 (2)
C1^{iv}—N1—C1	109.5 (3)	H4—C2—H5	113 (2)
N1—C1—H1	109.1 (19)	N1—C3—H6	111 (3)
N1—C1—H2	109.6 (18)	N1—C3—H7	110 (2)
H1—C1—H2	108 (3)	H6—C3—H7	112 (2)

Symmetry codes: (i) $-x, 1-y, z$; (ii) $x, 1-y, -z$; (iii) $-x, y, -z$; (iv) $\frac{1}{2}-x, \frac{1}{2}-y, z$.

unit cell of the room-temperature phase. The disordered sulfate tetrahedra are arranged in layers parallel to (001) so that ordered and disordered layers of sulfate are stacked in an alternating manner along [001].

7. Crystal structure of the cubic high-temperature phase

The high-temperature (HT) modification was investigated by Guinier–Simon X-ray powder diffraction. From a powder pattern recorded at 473 K a cubic crystal system with $a = 11.026$ (2) Å was determined [*TREOR*90 (Werner, 1990) and *Stadi P* software (Stoe, 1994)]. The reflection condition $h+k, h+l, k+l = 2n$ for hkl leads to the extinction symbol F- - -, thus, the space groups $F23$(196), $Fm\bar{3}$(202), $F\bar{4}32$(209), $F\bar{4}3m$(216) and $Fm\bar{3}m$(225) are possible. Assuming that the high-temperature phase is closely related to the pseudocubic room-temperature phase, a powder diffraction pattern was generated with tetramethylammonium cations ordered and all sulfate anions orientationally disordered. The space group $Fm\bar{3}m$(225) was chosen for the calculation, because it creates the highest restrictions to the symmetry of the $[N(CH_3)_4]^+$ cation. The resulting

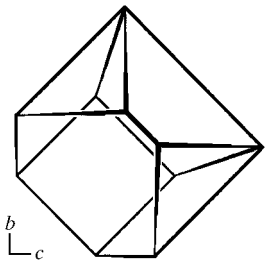

Planes {*hkl*}	Distances from center (mm)
{100}	0.14
{$\bar{1}\bar{1}1$}	0.12
{$\bar{1}11$}	0.15
{211}	0.12
{$\bar{1}\bar{1}1$}	0.17
{$1\bar{1}1$}	0.18
{$11\bar{1}$}	0.19
{$\bar{1}1\bar{1}$}	0.18

Fig. 4. Form of the RT-$[N(CH_3)_4]_2SO_4$ crystal.

Table 7. *Atomic parameters for the calculation of the HT-$[N(CH_3)_4]_2SO_4$ powder pattern*

Cubic, $a = 11.026$ Å, space group $Fm\bar{3}m$, $Z = 4$.

	Multiplicity/ Wyckoff letter	*x*	*y*	*z*	SOF
S1	4(*a*)	0.0	0.0	0.0	0.02083
N1	8(*c*)	1/4	1/4	1/4	0.04167
O1	32(*f*)	0.07600	0.07600	0.07600	0.04167
O2	24(*e*)	0.0	0.0	0.13200	0.04167
C1	32(*f*)	0.32800	0.32800	0.32800	0.16667
H1	96(*k*)	0.27145	0.38455	0.38455	0.50000

powder pattern fitted best with one N—C bond of a $[N(CH_3)_4]^+$ cation pointing towards $\frac{1}{2},\frac{1}{2},\frac{1}{2}$, that is the same orientation as in the room-temperature phase. For the disordered sulfate, it was neccessary to occupy 32(*f*) and 24(*e*) sites also with oxygen. Table 7 shows the atomic parameters used for the calculation and Table 8 the observed and calculated powder patterns in comparison. As the calculated pattern is already in good agreement with that observed, it is likely that the high-temperature form consists of free rotating sulfate tetrahedra in a fixed tetramethylammonium tetrahedra framework.

8. Structure relations

All $[N(CH_3)_4]_2SO_4$ phases can be derived from the Li_2O-type structure. If the low- and room-temperature unit cells are transformed as indicated by the thin lines in Fig. 6, the pseudocubic close packing of the SO_4^{2-} tetrahedra is obvious. The $[N(CH_3)_4]^+$ tetrahedra keep the same orientation throughout all phase transitions of $[N(CH_3)_4]_2SO_4$. In the low-temperature phase, however, deviation from the ideal cubic coordination of the

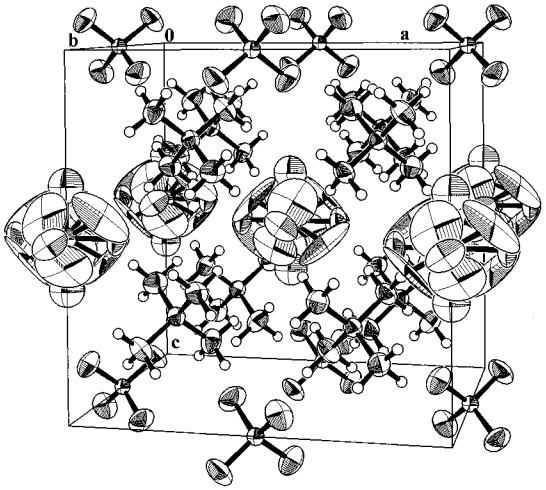

Fig. 5. *ORTEP*II (Johnson, 1971) plot (50% probability level) of the tetragonal RT-$[N(CH_3)_4]_2SO_4$ unit cell.

sulfate by eight $[N(CH_3)_4]^+$ cations is pronounced. In the room-temperature phase this deviation almost disappears. The high-temperature phase metrically represents the ideal cubic phase with all SO_4^{2-} tetrahedra orientationally disordered and surrounded by eight equidistant cations.

Whereas the relationship of the three phases and the Li_2O-type is obvious, an examination of symmetry relations is more complicated. The phases of $[N(CH_3)_4]_2SO_4$ are not connected by direct group–subgroup relations. Therefore, intermediate structures have to be found which are not realized, but enable a path from the high- to the room- and low-temperature phases by subsequent reduction of the symmetry. Fig. 7 shows the complete group–subgroup diagram following the rules proposed by Bärnighausen & Müller (1996).

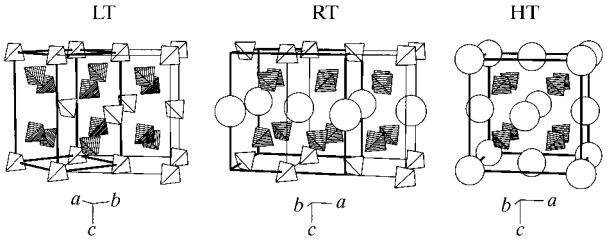

Fig. 6. Structural relation of the $[N(CH_3)_4]_2SO_4$ phases. Bold lines indicate the unit cells, $[N(CH_3)_4]$ tetrahedra are shaded, ordered SO_4 tetrahedra are represented by unshaded tetrahedra, disordered ones by unshaded spheres.

Starting with the cubic face-centered HT-$[N(CH_3)_4]_2SO_4$ ($Fm\bar{3}m$), all sulfate anions are crystallographically equivalent and disordered. For reasons of clarification, only the coordination of sulfur by O atoms in the form of a cube as the disorder model is regarded. Loss of all threefold axes results in the *translationengleiche* subgroup *I*4/*mmm* of index 3. The tetragonal body-centered lattice has only half the volume of the high-temperature phase, but the set of all (pure) translations is retained. All sulfate anions are still crystallographically equivalent and disordered. However, this structure is not realized, but space group $P4_2/nmc$ (LT-$[N(CH_3)_4]_2SO_4$) is a *klassengleiche* subgroup of index 2 of space group *I*4/*mmm*. Within this transformation two special Wyckoff positions 16(*n*) in space group *I*4/*mmm*, each occupied by C and O atoms, split into two special Wyckoff positions 8(*g*) in space group $P4_2/nmc$. Whereas C atoms occupy both new sites, only one site is occupied by O atoms. In structural terms this is the

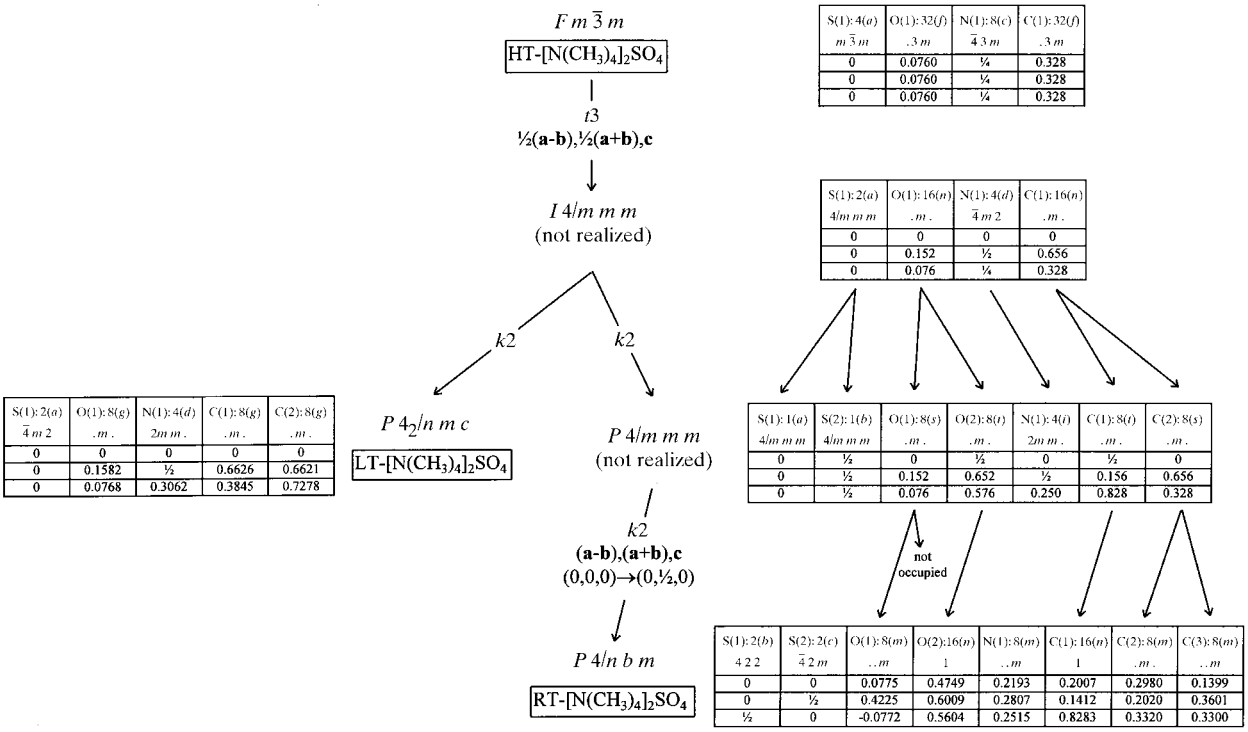

S(1): 4(*a*) $m\bar{3}m$	O(1): 32(*f*) .3 *m*	N(1): 8(*c*) $\bar{4}3m$	C(1): 32(*f*) .3 *m*
0	0.0760	¼	0.328
0	0.0760	¼	0.328
0	0.0760	¼	0.328

S(1): 2(*a*) 4/*m m m*	O(1): 16(*n*) .*m*.	N(1): 4(*d*) $\bar{4}m2$	C(1): 16(*n*) .*m*.
0	0	0	0
0	0.152	½	0.656
0	0.076	¼	0.328

S(1): 2(*a*) $\bar{4}m2$	O(1): 8(*g*) .*m*.	N(1): 4(*d*) 2*m m*.	C(1): 8(*g*) .*m*.	C(2): 8(*g*) .*m*.
0	0	0	0	0
0	0.1582	½	0.6626	0.6621
0	0.0768	0.3062	0.3845	0.7278

S(1): 1(*a*) 4/*m m m*	S(2): 1(*b*) 4/*m m m*	O(1): 8(*s*) .*m*.	O(2): 8(*t*) .*m*.	N(1): 4(*i*) 2*m m*.	C(1): 8(*t*) .*m*.	C(2): 8(*s*) .*m*.
0	½	0	½	0	½	0
0	½	0.152	0.652	½	0.156	0.656
0	½	0.076	0.576	0.250	0.828	0.328

S(1): 2(*b*) 4 2 2	S(2): 2(*c*) $\bar{4}2m$	O(1): 8(*m*) ..*m*	O(2): 16(*n*) 1	N(1): 8(*m*) ..*m*	C(1): 16(*n*) 1	C(2): 8(*m*) .*m*.	C(3): 8(*m*) ..*m*
0	0	0.0775	0.4749	0.2193	0.2007	0.2980	0.1399
0	½	0.4225	0.6009	0.2807	0.1412	0.2020	0.3601
½	0	-0.0772	0.5604	0.2515	0.8283	0.3320	0.3300

Fig. 7. Group–subgroup diagram for the three phases of $[N(CH_3)_4]_2SO_4$. 'Not realized' structure parameters are idealized and were calculated from the parameters of HT-$[N(CH_3)_4]_2SO_4$ *KPLOT* (Hundt, 1979). Note: parameters 0, $\frac{1}{2}$ and $\frac{1}{4}$ are fixed by symmetry, whereas free parameters are decimal (as in 0.0, 0.25, 0.51). For clarification, symmetrically equivalent atom positions were preferred on few occasions to those in the tables.

Table 8. *X-ray powder diffraction pattern for HT-$[N(CH_3)_4]_2SO_4$*

Miller indices, observed d_{obs} (Å) and calculated d_{calc} (Å) *d*-spacings (obtained from Guinier–Simon X-ray film, refined by least-squares methods), visually estimated and calculated intensities of the cubic phase at 473 K. The pattern was calculated using the program *THEO* (from *Stadi P* software; Stoe, 1994).

hkl	d_{obs}	d_{calc}	I_{obs}	I_{calc}
111	6.36582	6.365864	90	91.0
200	5.51296	5.513000	5	4.0
220	3.89825	3.898280	100	100.0
311	3.32444	3.324464	50	49.5
222		3.182932		0.2
400		2.756500		0.3
331	2.52952	2.529538	2	1.8
420	2.46547	2.465489	5	3.4
422	2.25066	2.250673	2	3.8
511		2.121955		0.3
333	2.12194	2.121955	5	6.2
440	1.94913	1.949140	2	2.4
531	1.86372	1.863734	5	5.7
600	1.83765	1.837667	2	1.2
442		1.837667		1.0
620		1.743364		0.2
533		1.681449		0.9
622		1.662232		0.5
444		1.591466		0.5
551		1.543949		0.8
711		1.543949		0.6
640		1.529031		0.0
642	1.47340	1.473411	5	4.3
553	1.43545	1.435463	2	0.9
731		1.435463		1.8

ordering of all sulfate anions, which are still crystallographically equivalent.

The space group *P*4/*nbm* (RT-$[N(CH_3)_4]_2SO_4$) can only be deduced from the space group *I*4/*mmm*, if an intermediate step to the *klassengleiche* subgroup *P*4/*mmm* of index 2 is made. The body-centering is ceased and the formerly crystallographically equivalent sulfate anions are now distinguishable. Nevertheless, all sulfate anions are still disordered. Again, this structure is not realized, but the space group *P*4/*nbm* (RT-$[N(CH_3)_4]_2SO_4$) is a *klassengleiche* subgroup of *P*4/*mmm* of index 2. The subgroup is obtained by enlarging the conventional cell ($\mathbf{a}' = 2\mathbf{a}$, $\mathbf{b}' = 2\mathbf{b}$, $\mathbf{c}' = \mathbf{c}$), resulting in the space group *C*4/*amd*, which becomes the space group *P*4/*nbm* (RT-$[N(CH_3)_4]_2SO_4$) after changing into a standard setting with a new origin choice. The complete cell transformation from space group *P*4/*mmm* to space group *P*4/*nbm* ($\mathbf{a}'' = \mathbf{a} - \mathbf{b}$, $\mathbf{b}'' = \mathbf{a} + \mathbf{b}$, $\mathbf{c}'' = \mathbf{c}$) includes doubling of the cell volume. For that reason the multiplicity of the Wyckoff positions has to change also. Whereas special Wyckoff position 8(*t*) in *P*4/*mmm* is transformed into the general Wyckoff position 16(*n*) in *P*4/*nbm*, the special Wyckoff position 8(*s*) splits into two special Wyckoff positions 8(*m*). The C atoms of the tetramethylammonium cation occupy both sites, but O atoms occupy only one of the two possible new sites. In terms of structure this is the ordering of one sulfate anion position.

Directly related to the reduction of symmetry during a phase transition is the appearance of twinning domains. This is not detectable with powder diffraction methods. However, cooling the single crystal from room temperature below 263 K could result in a twinned crystal. Indeed, a rapidly cooled single crystal has shown twinning in X-ray oscillation photographs. However, a very slow and controlled temperature change, as applied to the single crystal measured, favors homogeneous and, therefore, equilibrium conditions. Taking into account that the room-temperature phase with its disordered sulfate anion serves as an 'intrinsic' twinned phase, the formation of a low-temperature single crystal is possible.

The authors thank the Fonds der Chemischen Industrie for financial support.

References

Albert, B. & Jansen, M. (1995). *Z. Anorg. Allg. Chem.* **621**, 1735–1740.

Bärnighausen, H. & Müller, U. (1996). *Symmetriebeziehungen zwischen den Raumgruppen als Hilfsmittel zur straffen Darstellung von Strukturzusammenhängen in der Kristallchemie*. Institut für Anorganische Chemie, University of Karlsruhe, Germany.

Berg, R. W. (1978). *Spectrochim. Acta Part A*, **34**, 655–659.

Christe, K. O., Curtis, E. C., Dixon, D. A., Mercier, H. P., Sanders, J. C. P. & Schrobilgen, G. J. (1991). *J. Am. Chem. Soc.* **113**, 3351–3361.

Christe, K. O., Dixon, D. A., Mercier, H. P. A., Sanders, J. C. P., Schrobilgen, G. J. & Wilson, W. W. (1994). *J. Am. Chem. Soc.* **116**, 2850–2858.

Christe, K. O., Wilson, W. W., Wilson, R. D., Bau, R. & Feng, J. (1990). *J. Am. Chem. Soc.* **112**, 7619–7625.

Enraf–Nonius (1989). *CAD-4 Software*. Version 5.0. Enraf–Nonius, Delft, The Netherlands.

Gerhartz, W. (1987). Editor. *Ullman's Encyclopedia of Industrial Chemistry*, 5th ed., Vol. A8, pp. 493–504. New York, Weinheim: VCH Publishers.

Hundt, R. (1979). *KPLOT. Program for Plotting and Investigating Crystal Structures*. Updated Version 6.41. University of Bonn, Germany.

Husain, M. M. & Singh, D. K. (1984). *Synth. React. Inorg. Met.-Org. Chem.* **14**, 49–55.

Johnson, C. K. (1971). *ORTEP*II. Report ORNL-3794, revised. Oak Ridge National Laboratory, Tennessee, USA.

Kabisch, G. (1980). *J. Raman Spectrosc.* **9**, 279–285.

Kopf, J. & Ruebcke, H.-C. (1993). *CADSHEL*3.1. *Program for Data Reduction*. University of Hamburg, Germany.

Markowitz, M. M. (1957). *J. Org. Chem.* **22**, 983–984.

Nakamoto, K. (1986). *Infrared and Raman Spectra of Inorganic and Coordination Compounds*, 4th ed. New York: Wiley-Interscience.

Sato, S., Endo, M., Hara, N., Nakamura, D. & Ikeda, R. (1995). *J. Mol. Struct.* **345**, 197–203.

Sheldrick, G. M. (1976). *SHELX*76. *Program for Crystal Structure Determination*. University of Cambridge, England.

Sheldrick, G. M. (1985). *SHELXS*86. *Program for the Solution of Crystal Structures*. University of Göttingen, Germany.

Sheldrick, G. M. (1993). *SHELXL*93. *Program for the Refinement of Crystal Structures.* University of Göttingen, Germany.

Stoe (1994). *Stadi P software Visual Xpow*2.29. Germany.

Werner, P.-E. (1990). *TREOR*90. *Trial and Error Program for Indexing of Unknown Powder Patterns*. University of Stockholm, Sweden.